Microstructure and Crack Distribution of Fe-based Amorphous Alloys Manufactured by Selective Laser Melting

Yuanjie Zhang, Bo Song*, Lei Zhang, Zhiwei Wang, Yusheng Shi

State Key Laboratory of Materials Processing and Die & Mould Technology,

Huazhong University of Science and Technology, Wuhan 430074, China

Abstract: In this study, Fe-based amorphous alloys with a length and width of 10 mm and height of 6 mm were prepared by selective laser melting (SLM). X-ray diffraction, Differential Thermal Analysis and Scanning Electron Microscope were used to investigated the effect of scan space and strategy on the crystallization, microstructure, crack distribution and density. The content of amorphous calculated by Differential Thermal Analysis is up to 93%. There is an obviously trend to lower crack distribution and higher density with an appropriate scan spaces and strategies. With the increasing scan space, the density increased first, then gradually decreased, while the crack decreased and then increasing with the scan space.

Keywords: selective laser melting, amorphous alloys, crack

1 Introduction

Bulk metallic glasses (BMG), which have a short-range order and long range disorder structure, present an excellent mechanical property, physical property, chemical property and corrosion resistance. In 1960, the slice of Au-Si composition was achieved through rapidly solidifying by Duwez [1]. Since then, numbers of alloy compositions in different alloy systems were synthesized in the glass state [2-9]. A large variety of techniques are used to process BMG, such as melt spinning, water-quenching method, high-pressure die casting, copper mold casting and so on.

In this study, a new technology, selective laser melting (SLM), was applied in processing BMG. SLM, as one of the techniques with development potential in additive manufacturing (AM), was used to process varieties of metal alloys. Because

Corresponding authors. Tel.: +86 15927261681.
E-mail addresses: bosong@hust.edu.cn (B. Song)

the solidification occurs relatively quickly during SLM and generally reaches values on the order of 10^3–10^4 K/s [10], the local intrinsic cooling rate can be high enough to satisfy the critical cooling rate. Besides, for its short processing cycle, low costs, high design flexibility, and superior performance for produce parts. SLM has been applied in many alloys and composites.

Recently, some of BMG has been produced by SLM. The influence of laser power on densification, microstructure and mechanical properties of $Al_{86}Ni_6Y_{4.5}Co_2La_{1.5}$ scan tracks were systematically investigated by X. P. Li [11]. The results showed that high thermal stress in high laser power and low strength in low laser power will both cause the formation of cracks. Besides, the enhanced thermal fluctuation in high laser power also result in inhomogeneous chemical distribution and further severe crystallization. To deal with the cracks, X. P. Li studied the use of a re-scanning strategy during the selective laser melting [12]. It indicated that a high power initial scan followed by a lower power re-scan can relief the stress and reduce cracks. K. G. Prashanth processed $Al_{85}Nd_8Ni_5Co_2$ samples by SLM, which has a high compressive strength (1-0.5 GPa) at elevated temperatures (303-573 K) due to submicro-sized stable intermetallic phase dispersed in an Al matrix [13]. Hyo Yun Jung has investigated the microstructure, thermal stability and soft magnetic properties of Fe-based bulk metallic glasses with different parameters [14]. It shows that the samples with fully amorphous, good magnetic softness and high relative densities up to 99.7% can be fabricated by low v and high P. Zr-based bulk metallic glasses prepared by SLM or laser solid forming (LSF) were also studied [15-17]. It shows that large scale, complex and fully dense crack-free Zr-based bulk metallic glasses with high hardness, high compressive strength and small amount of ductility can be achieve using selective laser melting.

However, there are still a lot of problems in processing BMG, such as crystallization, integrality and cracks. In this study, the microstructure and crack distribution of Fe-based bulk metallic glasses with different scan strategy and scanning space manufactured by SLM was studied.

2 Experimental procedures

2.1 Powder feedstock

A master alloy with nominal composition $Fe_{43.7}Co_{7.3}Cr_{14.7}Mo_{12.6}C_{15.5}B_{4.3}Y_{1.9}$ (at.%) was prepared under N_2 atmosphere by gas atomization. Fig.1(a) shows the morphology of Fe-based metallic glasses and the particles are rod-like. The inset image in Fig. 1(a) state the XRD image of the powder. It is shown that the amorphous of the powder is good. While, Fig.1(b) shows the particle size distribution of the powder. The distribution accord with Gaussian distribution and the average particle size are 29 μm.

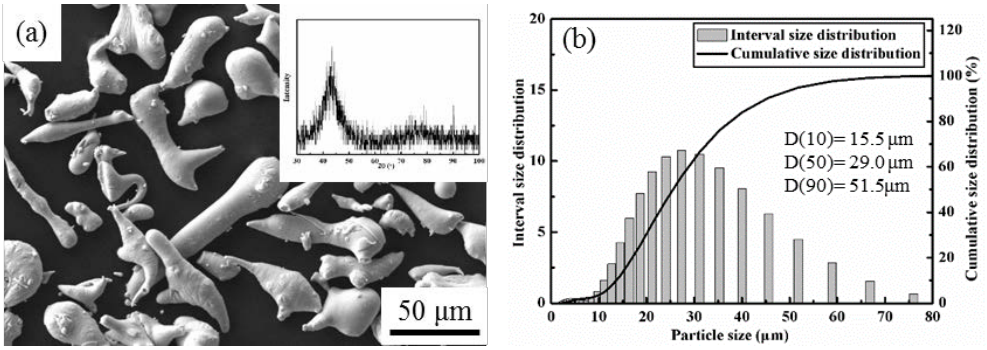

Fig. 1. (a) Morphology and (b) particle size distribution of Fe-based metallic glasses

2.2 SLM process

All parts were made on the EOS M280 SLM machine. This SLM installation is equipped with an Yb: YAG fibre laser, which can reach a maximum power of 400 W in continuous mode. The intensity distribution can be assumed to be Gaussian. Based on a series of preliminary experiments, the SLM parameters were fixed as follows: laser power of 150 W, scanning speed of 1000 mm/s, layer thickness of 0.04 mm. Then the hatch spacing and scan strategy were changed. The hatch spacing spread from 0.08 to 1.16 mm. There are three scan strategies, as shown in Fig.2(a). The scanning direction is rotated respectively by 0°, 90° and 67° after each layer, corresponding to strategy (1), (2) and (3). Bulk specimens with dimensions of 10 mm × 10 mm × 5 mm were produced, as shown in Fig. 2(b).

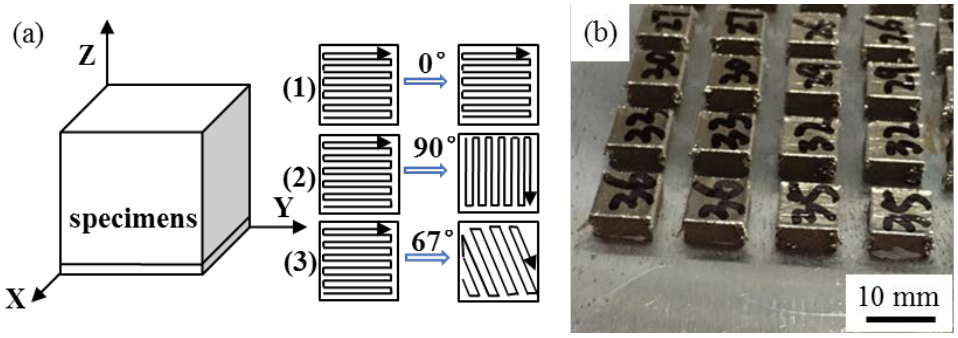

Fig. 2. (a) the three different strategies of SLM process; (b) SLM-processed specimens

2.3 Microstructural characterization

The phases of the bulk specimens were identified through X-ray diffraction (XRD-7000) analyses, which were performed with a Cu K_α radiation source at 40 kV and 30 mA; the continuous scan mode was used and the scan rate was 5°/min.

The DTA was used to detect the amorphous content. For calculate the content, the enthalpies of bulk are compared to powder.

Metallographic samples were prepared as per the standard procedures and were etched with aqua regia for 30 s. Microstructural analysis was carried out by scanning electron microscope (SEM) equipped with energy dispersive X-ray analysis (EDX) detectors.

2.4 Mechanical properties

The porosity calculated by 10 pictures of specimen morphology were used to express the density of specimens. The crack rate defined by crack area ratio was calculated by 10 pictures of specimen morphology, too.

Nanoindentation tests on the polished sections of SLM parts were performed using a TI750 nanoindentation tester (Hysitron, America) at room temperature. A loading–unloading test mode was used and a test force 6000 μN, a loading speed 1.200 mN/s and a hold time 2 s were chosen.

3 Results and discussion

3.1 Different scanning space

3.1.1 Phase identification

The thermal stability and crystallization behavior of the different samples was assessed by DTA and the results are shown in Fig. 3. All specimens exhibit a distinct glass transition followed by a multi-stage crystallization process. It is proved that the glass transition occurred and the specimens contains an amorphous phase. Compared specimens with different scanning space, specimen with middle space (0.12 mm) has a highest amorphous phase, up to 93.2%.

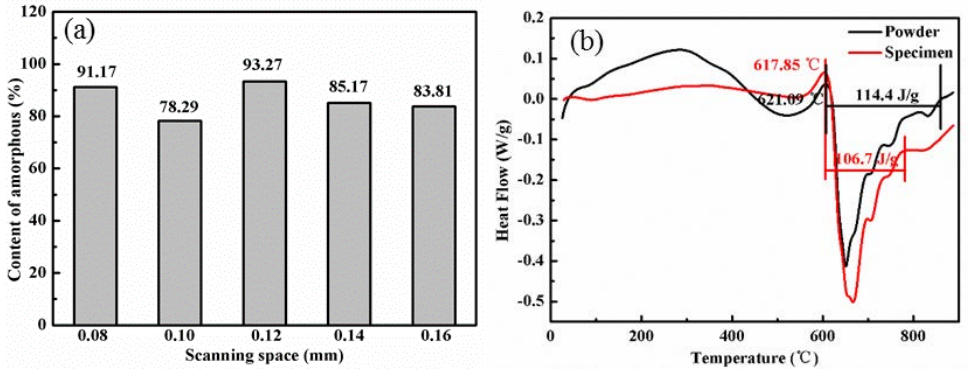

Fig.3 (a) The amorphous content of bulk with different scanning space; (b) differential thermal analysis of powder and specimen with 0.12 mm

3.1.2 Microstructure evolution

Fig. 4 shows the microstructure of specimens with different scanning space. The middle parameters are studied. Metallographic samples were prepared as per the standard procedures and were etched with aqua regia for 30 s. As shown in Fig. 4(a)(c)(e), the crystallization tends to emerge near the crack. Besides, compared to others, the crystallization areas of specimen with middle space (0.12 mm) is smaller. The result is consistent with the DTA.

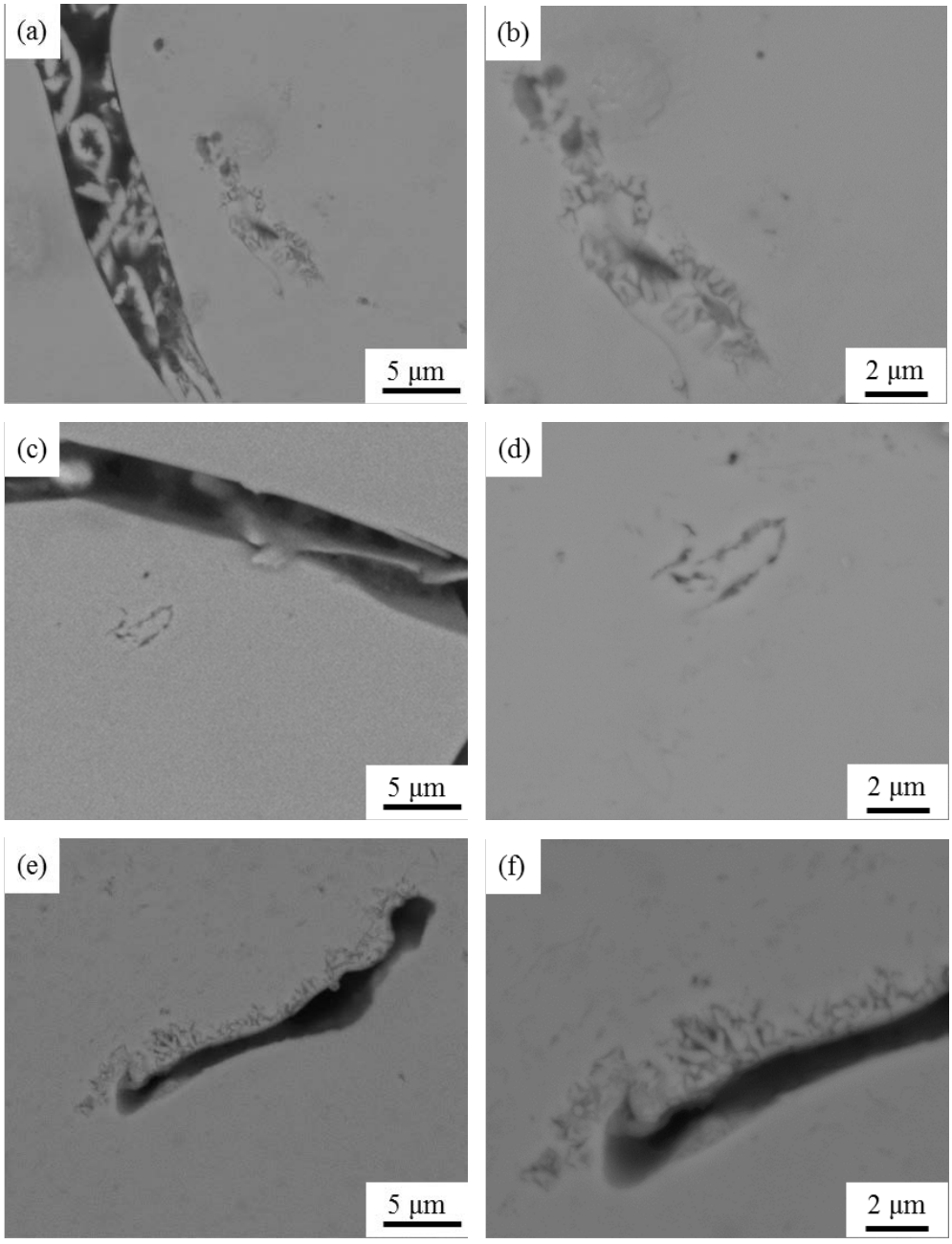

Fig.4 Microstructure and magnification with different scanning space: (a)(b) 0.10 mm; (c)(d) 0.12 mm; (e)(f) 0.14 mm

3.1.3 Mechanical properties

The crack distribution, crack rate and density are shown in Fig. 5. It shows that there are lots of crisscross cracks, this is due to the brittleness of Fe-based metallic glasses.

The crack rate decreased with the increasing scanning space first. With the further increasing space, it then increased quickly. When the scanning space is 0.12 mm, the crack rate is 0.66%, which is lower than others.

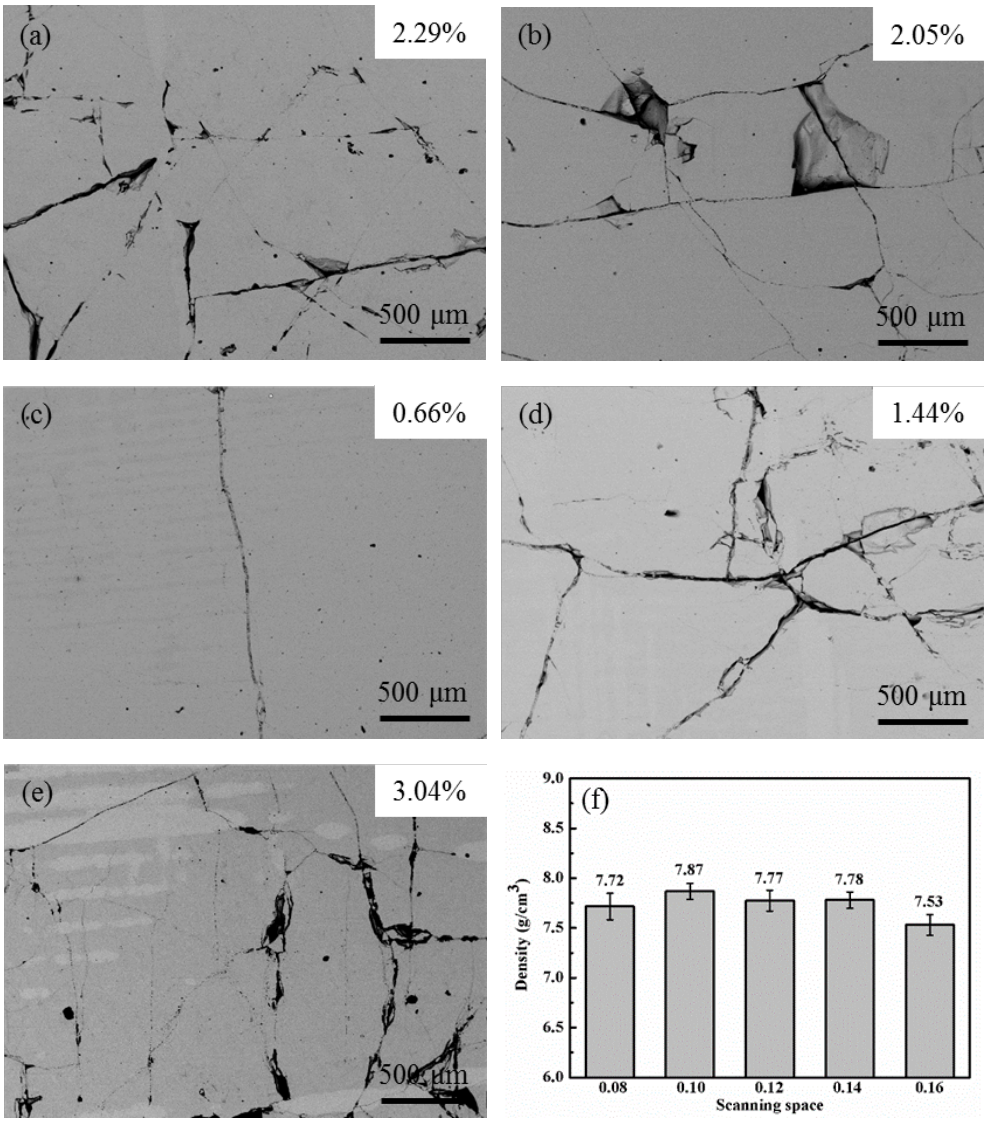

Fig.5 Specimens with different scanning space range from 0.08-0.16 mm: (a)-(e) the morphology and crack rate; (f) density

It is obviously that the scanning space relates to the overlap rate, which is defined as:

$$\eta=\left(1-\frac{S}{W}\right)\times 100\% \quad (1)$$

The width of pool (W) and scanning space (S) are shown in Fig. 6.

While the space is too low, high overlap rate means the number of laser scanning increased, result in more crystallization and cracks. However, the lower overlap rate will cause a lot of pores and department of specimens, which will also lead to cracks. In this study, specimen with 31% overlap rate exhibit a higher performance, which is corresponding with the study of Li Wang [18].

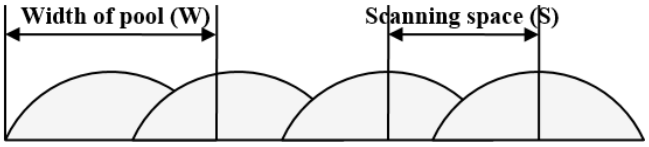

Fig.6 Diagrammatic sketch of width of melting pool and scanning space

3.2 Different scanning strategy

One of the parameter was chosen to compared the influence of strategy. Fig. 7 shows the crack distribution, crack rate and phases analysis of three strategies which are shown in Fig. 2(a). Fig. 7(d) shows that all of the specimens has an amorphous phase. It is illustrated that the crack rate of strategy (2) is better than others, while the crack rate of strategy (3) is the worst.

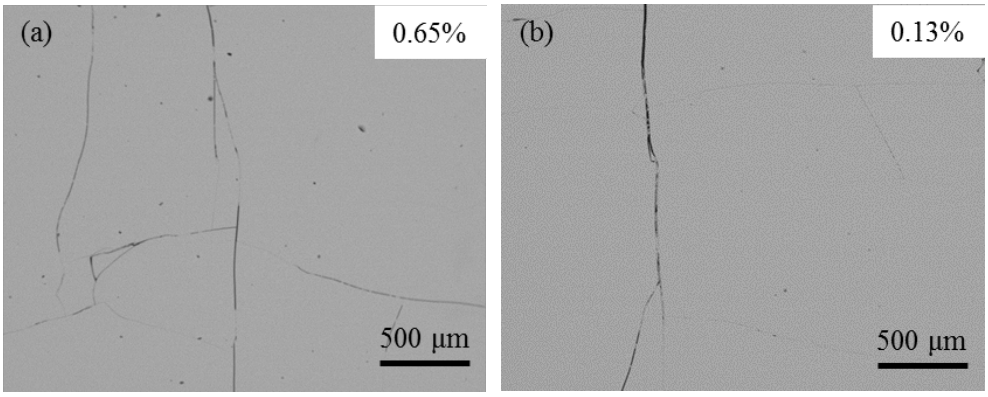

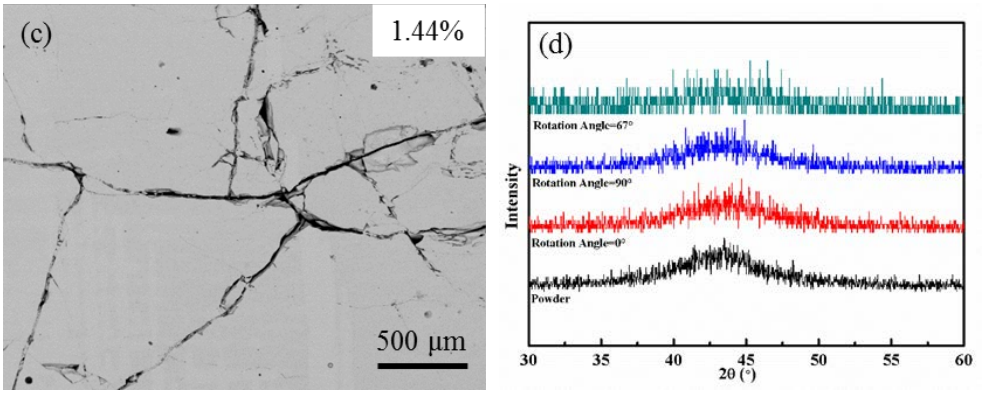

Fig.7 Specimens with different scanning strategies: (a)-(c) crack distribution of strategy (1)-(3); (d) phase analysis

The nanohardness of three strategies which are shown in Fig. 8. The nanohardness results that the hardness increased with strategy (1) to (3), up to 17.2 GPa, which is higher than the as-cast glassy samples (1253 HV) [19].

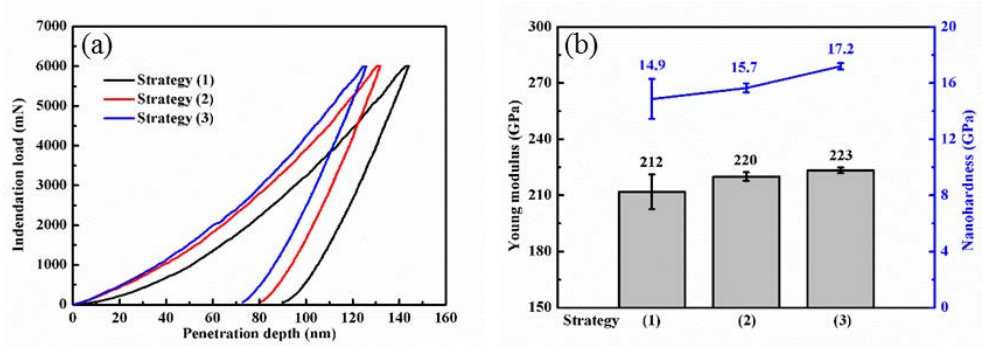

Fig.8 (a) loading-penetration depth curves and (b) nanohardness for nano-indentation of different scanning strategies samples

4 Conclusions

Fe-based bulk metallic glasses has been produced by SLM with different scanning space and strategies. The main conclusions of the present study, which might be helpful for other laser-powder-based AM technologies and for amorphous alloys materials, are as follows:

(1) Specimen with a 0.12 mm scanning space has a highest amorphous phase, up to 93.2%.

(2) Due to the brittleness of Fe-based metallic glasses, there are lots of crisscross cracks. But the crack rate reduced to 0.66% when the scanning space is 0.12 mm, which is much lower than others.

(3) It is illustrated that the crack rate of strategy (2) is better than others. However, the nanohardness of strategy (3) is the highest, up to 17.2 GPa, which is higher than the as-cast glassy samples (1253 HV).

Acknowledgments

This work was supported by the National Natural Science Foundation of China (Grant No. 51531003, 51505166).

References

[1] Klement W, Willens R H, Duwez P O L. Non-crystalline structure in solidified gold–silicon alloys[J]. Nature, 1960, 187(4740): 869-870.

[2] Luborsky F E. Amorphous metallic alloys[M]. Butterworth and Co (Publishers): London, UK, 1983.

[3] Anantharaman T R. Metallic glasses: production, properties and applications[J]. Trans Tech Publications SA, Trans Tech House, CH-4711 Aedermannsdorf, Switzerland, 1984. 302, 1984.

[4] Liebermann H H. Rapidly solidified alloys: processes, structures, properties, applications[J]. Marcel Dekker, Inc, 270 Madison Ave, New York, New York 10016, USA, 1993. 788, 1993.

[5] Suryanarayana C, Inoue A. Bulk metallic glasses[M]. Boca Raton, FL: CRC press, 2011.

[6] Suryanarayana C. Rapidly quenched metals, a bibliography, 1973-1979[M]. Ifi/Plenum, 1980.

[7] Anantharaman T R, Suryanarayana C. Review: A decade of quenching from the melt[J]. Journal of Materials Science, 1971, 6(8): 1111-1135.

[8] Jones H, Suryanarayana C. Rapid quenching from the melt: An annotated bibliography 1958–72[J]. Journal of Materials Science, 1973, 8(5): 705-753.

[9] Chen H S. Glassy metals[J]. Reports on Progress in Physics, 1980, 43(4): 353.

[10] Zheng B, Zhou Y, Smugeresky J E, et al. Processing and behavior of Fe-based metallic glass components via laser-engineered net shaping[J]. Metallurgical and Materials Transactions A, 2009, 40(5): 1235-1245.

[11] Li X P, Kang C W, Huang H, et al. Selective laser melting of an Al 86 Ni 6 Y 4.5 Co 2 La 1.5 metallic glass: processing, microstructure evolution and mechanical properties[J]. Materials Science and Engineering: A, 2014, 606: 370-379.

[12] Li X P, Kang C W, Huang H, et al. The role of a low-energy–density re-scan in fabricating crack-free Al 85 Ni 5 Y 6 Co 2 Fe 2 bulk metallic glass composites via selective laser melting[J]. Materials & Design, 2014, 63: 407-411.

[13] Prashanth K G, Shahabi H S, Attar H, et al. Production of high strength Al 85 Nd 8 Ni 5 Co 2 alloy by selective laser melting[J]. Additive Manufacturing, 2015, 6: 1-5.

[14] Jung H Y, Choi S J, Prashanth K G, et al. Fabrication of Fe-based bulk metallic glass by selective laser melting: a parameter study[J]. Materials & Design, 2015, 86: 703-708.

[15] Li X P, Roberts M P, O'Keeffe S, et al. Selective laser melting of Zr-based bulk metallic glasses: Processing, microstructure and mechanical properties [J]. Materials & Design, 2016, 112: 217-226.

[16] Zhang Y, Lin X, Wang L, et al. Microstructural analysis of $Zr_{55}Cu_{30}Al_{10}Ni_5$ bulk metallic glasses by laser surface remelting and laser solid forming [J]. Intermetallics, 2015, 66: 22-30.

[17] Zhang Y, Lin X, Wei L, et al. Influence of powder size on the crystallization behavior during laser solid forming $Zr_{55}Cu_{30}Al_{10}Ni_5$ bulk amorphous alloy [J]. Intermetallics, 2016, 76: 1-9.

[18] Li Wang. Reserch on the performance in selective laser melting of metallic part [D]. Wuhan: Huazhong University of Science and Technology, 2013.

[19] Shen J, Chen Q, Sun J, et al. Exceptionally high glass-forming ability of an FeCoCrMoCBY alloy[J]. Applied Physics Letters, 2005, 86(15): 151907.